Int. J. Environ. Res., 7(1):173-186, Winter 2013
ISSN: 1735-6865

Numerical Simulation on Wind Flow over Step-shaped Cliff Topography with Rough Surface

Yassin, M.F.[1,2*] and Al-Harbi, M.[1]

[1] Department of Environmental Technology Management, Kuwait University, Kuwait

[2] Faculty of Engineering, Assiut University, Egypt

Received 20 April 2012; Revised 4 Aug. 2012; Accepted 17 Aug. 2012

ABSTRACT: To enhance the understanding of the impact of obstacle buildings on pollution transportation and dispersion in the atmospheric boundary layer, it is necessary to know the atmospheric flow characteristics over terrains. Wind flow characteristics in a boundary layer over a step-shaped cliff topography model with rough and smooth surfaces were studied numerically using Computational Fluid Dynamics models (CFD). The CFD models that were used for the simulation were based on the steady-state Reynolds-Average Navier-Stoke equations (RANS) with turbulence models; standard and RNG models. The rough surface was modeled using windbreak fence, which was set on the step-shaped cliff model surface. The results of the numerical model were validated against the wind tunnel results in order to optimize the turbulence model. Numerical predictions agreed reasonably with the wind tunnel results. The results indicated that rough surface has a great influence on the turbulent flow characteristics and vortex rotating. The wind velocity for rough surface near the ground level was observed to be lower than that for the smooth surface of the step-shaped cliff model. Large flow separations were formed by the windbreak fences. Distortion of the flow at the windward corner of the step created a steep gradient of velocity and large turbulent mixing.

Key words: Atmospheric turbulence,CFD models, Rough surface,Terrain model,Wind flow

INTRODUCTION

Wind flow above complex terrain has become one of the most important topics of environmental research. This is because wind turbines are increasingly erected in areas with complex orography, furthering the course of wind energy is the main impetus for the investigation. Good knowledge of the flow over complex terrain is essential for precisely estimating wind energy potential, assessing structural loads on turbines. An understanding of flow in complex terrain is also crucial for the parameterization of form drag in meteorological models. It is also significant for various dispersion applications. Several studies have paid a great deal of attention to atmospheric boundary layer flow over hills. Jackson and Hunt (1975) presented their two-dimensional (2D) analysis of turbulent flow in complex terrain, which was later extended to three-dimensional (3D) flow by Mason and Stykes (1979). This theory has been refined and implemented numerically into commercial codes such as MS3DJH, MSFD and WAsP (Taylor et al. 1983; Walmsley et al. 1986; and Beljaars et al. 1987). These so-called linear models have the advantage of producing computationally fast and accurate results for terrains of gentle slopes of less than 0.3 or 17æ% (Wood 1995; Walmsley and Taylor 1996). Until recently, many investigators have attempted to measure turbulence in the backward-facing step flow with sophisticated experimental techniques (Eaton and Johnston, 1981). However, there are relatively fewer studies on wind flow over step-shaped topography with turbulent boundary layer (Bowen and Lindley, 1977; Adams and Johnston, 1988; Friedrich and Arnal, 1990; Djilali and Gartshora, 1991; Kasagi and Matsunaga, 1993; Olsson, 1999). William and Joseph (2000) evaluated the viability of using a step-shaped terrain representation of a smooth mountain profile in model simulations of small-amplitude mountain waves, where the result can be compared against known analytic solutions. Ross et al. (2004) have performed numerical and experimental studies in order to assess the performance of different turbulence closure schemes in predicting the flow field over a hill. Two-dimensional steep hills of different slopes, in both neutral and stably stratified flow conditions were studied. Loureiro and Freire (2005) have investigated the effects that a large change in

*Corresponding author E-mail: mohamed_f_yassin@hotmail.com

surface elevation provokes on the properties of the atmospheric using wind tunnel and water channel experiments. Mouzakis and Bergels (2005) present predictions of the two-dimensional turbulent flow over a triangular ridge. Turbulent boundary layer with a step change in surface roughness was investigated experimentally by Krogstad and Nickels (2006). Poggia et al. (2007) collected a new data set above a terrain of gentle hills to explore experimentally and theoretically the 2-D structure of the mean velocity. Blocken et al. (2007) addressed the problem of horizontal homogeneity associated with the use of sand-grain roughness wall functions. This is done by focusing on the CFD simulation of a neutrally stratified, horizontally homogeneous atmospheric boundary layer flow over uniformly rough, flat terrain.

This paper presents the results of numerical investigatation for studying the effect of the rough surface on the wind flow in the turbulent boundary layer over step-shaped cliff topography. Therefore, the aim of the present work is to improve the understanding of mechanism of simulation on the wind flow over terrain topography and to predict the wind flow over local topography. For this purpose, a two-dimensional model of step-shaped cliff with and without obstacles fence was considered. Mean velocity, turbulence intensity and turbulent kinetic energy were analyzed and discussed at different locations in the downwind distance over step-shaped cliff model under neutral atmospheric conditions.

MATERIALS & METHODS

In this paper, the numerical simulations were performed using the FLUENT CFD code (Fluent, 2009), which is based on the finite volume method to solve the equations of conservation for the different transported quantities in the atmospheric flow (mass, momentum and energy). The code first performs the coupled resolution of the pressure and velocity fields and then evolution of other parameters.

A two-dimensional step-shaped cliff configuration was chosen as a model of steep curvature obstacles. The model geometry is shown in Fig. 1. In this figure, Z' means the height from the upper surface of the step-shaped cliff. The step-shaped cliff model is modeled on a 1:1000 scale. The geometry chosen was identical to that examined experimentally in a wind tunnel study by Yassin et al. (2001), where the cliff height was 75 m high in the real scale and its length was 20H (H=75 mm). The simulated rough surface was modeled with windbreak fence and the simulated smooth surface modeled without windbreak fence. The windbreak fence was set on the step-shaped cliff model surface. The computational domain was 3 m long x 1.8 m high, which was discretised as 109 x 50 grids. The model edge distance 7H from the inlet domain, 13.33H from the outlet domain, and 29.33H from the upper domain. Extensive tests of the grid intervals are carried out with increasing grid interval until further refinement is shown to be less significant. The computational mesh employed was a conventional non-uniform mesh, for which the optimal mesh was identified, consisting of 634675 cells of average side sizes. The origin of the domain was defined at the center of the front edge of the step-shaped cliff model. The expansion ratio in the non-uniform grid was 1.1. The grid intervals near the obstacles in the x-, and z-directions are Δx =0.16H, and Δz = 0.12H respectively. Fine cells were defined over the step-shaped cliff model, where high gradients were expected, and coarse cells elsewhere. A mesh refinement test was performed to identify the optimal mesh resolution and ensure the results were mesh-independent. To minimize truncation error, cell-size increments were gradual and limited to a maximum increment of 25% between contiguous cells. In Fluent, The grid was generated using GAMBIT software. The computational grid configurations over the step-shaped cliff model with and without obstacle fence are shown in Fig. 2.

The FLUENT CFD package has been configured to solve the Navier Stokes equations for the flow over the step-shaped cliff using the standard k-ε turbulence model (Launder and Spalding, 1974) and RNG k-ε turbulence model (Yakhot *et al.,* 1992) for computational efficiency and accuracy. The RNG k-ε model differs from the standard k-ε turbulence scheme only through the modification to the equation for ε, which includes an additional sink term in the turbulence dissipation equation to account for non-equilibrium strain rates and employs different values for the model coefficients (Kim and Baik, 2004). The governing equations of the model are shown below

Continuity equation

$$\frac{\partial u_i}{\partial x_i} = 0 \qquad (1)$$

Momentum equation

$$\frac{\partial u_i}{\partial t} + \frac{\partial}{\partial x_j}(u_j u_i) = -\frac{1}{\rho}\frac{\partial p}{\partial x_i} + \frac{\partial}{\partial x_j}\left\{\nu\left(\frac{\partial u_i}{\partial x_j} + \frac{\partial u_j}{\partial x_i}\right) - \overline{u_i' u_j'}\right\} \qquad (2)$$

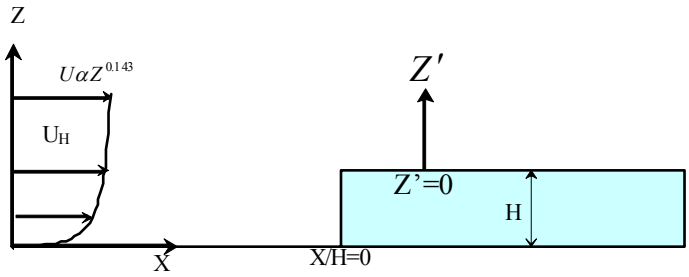

Fig. 1. Two-dimensional step-cliff model

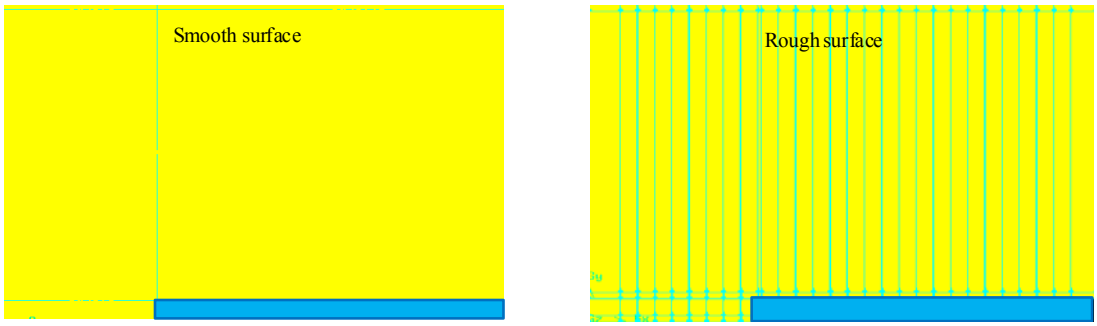

Fig. 2. the computational step-cliff configuration

T_{ke} - transport equation

$$\frac{\partial K}{\partial t}+\frac{\partial K u_i}{\partial x_i}=\frac{\partial}{\partial x_i}\left(\frac{\nu_t}{\sigma_k}\frac{\partial K}{\partial x_i}\right)+\nu_t\left(\frac{\partial u_i}{\partial x_j}+\frac{\partial u_j}{\partial x_i}\right)\frac{\partial u_i}{\partial x_j}-\varepsilon \tag{3}$$

ε - transport equation for standard k-ε turbulence model

$$\frac{\partial \varepsilon}{\partial t}+\frac{\partial \varepsilon u_i}{\partial x_i}=\frac{\partial}{\partial x_i}\left(\frac{\nu_t}{\sigma_\varepsilon}\frac{\partial \varepsilon}{\partial x_i}\right)+c_{1\varepsilon}\frac{\varepsilon}{K}\nu_t\left(\frac{\partial u_i}{\partial x_j}+\frac{\partial u_j}{\partial x_i}\right)\frac{\partial u_i}{\partial x_j}-c_{2\varepsilon}\frac{\varepsilon^2}{K} \tag{4}$$

ε - transport equation for RNG k-ε turbulence model

$$\frac{\partial \varepsilon}{\partial t}+\frac{\partial \varepsilon u_i}{\partial x_i}=\frac{\partial}{\partial x_i}\left(\frac{\nu_t}{\sigma_\varepsilon}\frac{\partial \varepsilon}{\partial x_i}\right)+c_{ls}\frac{\varepsilon}{K}\nu_t\left(\frac{\partial u_i}{\partial x_j}+\frac{\partial u_j}{\partial x_i}\right)\frac{\partial u_i}{\partial x_j}-c_{2\varepsilon}\frac{\varepsilon^2}{K}-R \tag{5}$$

$$R=c_\mu\eta^3\varepsilon^2\frac{1-\eta/\eta_0}{k(1+\beta_0\eta^3)} \tag{6}$$

$$\eta=\frac{K}{\varepsilon}\left\{\left(\frac{\partial u_i}{\partial x_j}+\frac{\partial u_j}{\partial x_i}\right)\frac{\partial u_i}{\partial x_j}\right\}^{1/2} \tag{7}$$

$$-\overline{u_i'u_j'}=\nu_t\left(\frac{\partial u_i}{\partial x_j}+\frac{\partial u_j}{\partial x_i}\right)-\frac{2}{3}K\delta_{ij} \tag{8}$$

$$\nu_t=c_\mu\frac{K^2}{\varepsilon} \tag{9}$$

where, u_i is the *i*th mean velocity component; *p* is the deviation of pressure from its reference value and ρ is the air density. v_t is the turbulent viscosities of momentum, respectively, δij is the kronecker delta. *v* is the kinematic viscosity of air. η =4.38 and β_0 = 0.012. Table 1 show the constant values in the transport equations.

In modeling atmospheric flow, smaller grid size is desirable near the surface of the step-shaped cliff model to better resolve flow, but away from the model, a larger grid size is allowable. The governing equations set was solved numerically on a staggered grid system using the finite-volume following the semi-Implicit Method for pressure-Linked Equation (SIMPLE) algorithm described by Patankar (1980). The standard and RNG k-ε turbulence models were employed here for comparison because of its widespread acceptance in diverse fields.

Velocity inlet boundary layer conditions were used in the main inlet wind flow. The initial wind speed is uniform (10 m/s) with low turbulence intensity. A user-defined subroutine for including the turbulence 0.143 the power law in rural area inlet velocity profile into FLUENT code was developed and used in the analysis. The initial condition for wind velocities, turbulent kinetic energy, *K* and its dissipation rate ε are specified as (FLUENT, 2009)

$$U = U_H \left(\frac{Z}{Z_H} \right)^n \tag{11}$$

$$K = \frac{u_\tau^2}{\sqrt{c_\mu}} \tag{12}$$

$$\varepsilon = \frac{c_\mu^{3/4} (T_{Ke}^{3/2})}{l} \tag{13}$$

where, U_H is the velocity at a height Z_H ; *Z* is the height above the ground, and n is the power exponent, u_τ is the friction velocity and *l* is the turbulence length scale. The ground and step-shaped cliff surfaces are defined as walls with no-slip boundary condition. The wall boundary conditions for momentum are applied to all solid surface and rough walls. Zero gradient boundary conditions are applied at the outflow and upper boundaries.

The experimental data was used for the validation of numerical simulation obtained from a detailed wind tunnel study by Yassin et al. (2001). Experiments were performed in a closed-circle boundary layer wind tunnel, which is shown in Fig.3. The width and height of the test section were 2.2 and 1.5 m. A neutral stratified atmospheric boundary layer was simulated using three spires, one 90 mm high cubic array placed just downstream of the contraction exit and followed by 60 and 30 mm cubic roughness element, covering 10.2 m of the test-section floor. This arrangement was employed to generate a thick turbulent boundary layer as the approaching flow. Reynolds number based on U_H and H is 3.5 x 10^4. Fig. 4 shows the simulated turbulent boundary layer profile at X=0.0 corresponds to the center of the step model. Tripping wires (1 mm rectangular columns, 50 mm intervals) were arranged over the step-shaped cliff. The windbreak fence over the step-shaped cliff was a solid plate fence, and was positioned at intervals of 50 mm, the same as for the tripping wires.

Wind velocity was measured using a hot wire Constant Temperature Anemometer (CTA) system with a split fiber probe, which was 70 μm diameter and 1.25 mm long. This was because the X-wire probe anemometers for turbulence measurement cannot give reasonable accuracy when the turbulence intensity is larger than 0.3 (Ishihara, 1999). Wind velocity measurements over the step-shaped model were made with split-fiber probe (55R55) in conjunction with a 90N10 DANTEC constant temperature anemometer system. The mean velocity was normalized by the reference velocity, U_H which is the velocity of the step-shaped cliff height. The velocity profiles were measured at the positions over the step-shaped cliff surface shown in Fig. 5. To clarify the change in the flow characteristics, the simulated data were interpolated at the same grid points as in the wind tunnel experiment. Smoke flow visualization was done in the wind tunnel to see what kind of flow characteristics appeared around the windward corner and over the step-shaped cliff model. The numerical results of the wind tunnel experiments for the flow structure were compared using the flow visualization and streamlines around the windward corner and over the step-shaped cliff model, as is shown in Fig 6. On the windward corner of the step-shaped cliff, the flow separation was created. A reattachment point appeared over the step-shaped cliff and moved downstream towards the downwind street. The numerical simulation of the wind flow was therefore consistent and in agreement with the measurements used in wind tunnel experiments.The simulated data was interpolated at the same grid points as in the wind tunnel experiment. The numerical data of the standard and RNG k-ε turbulence models was validated against the data obtained from the wind tunnel experiments at various locations. Figs. 7-8 show the vertical profiles of the normalized horizontal velocity for the surfaces with and without

Table 1. Constants in the turbulence models

Models	c_μ	$c_{1\varepsilon}$	$c_{2\varepsilon}$	σ_k	σ_ε
standard κ-ε model	0.09	1.44	1.92	1.0	1.3
RNG κ-ε model	0.085	1.42	1.68	0.7179	0.7179

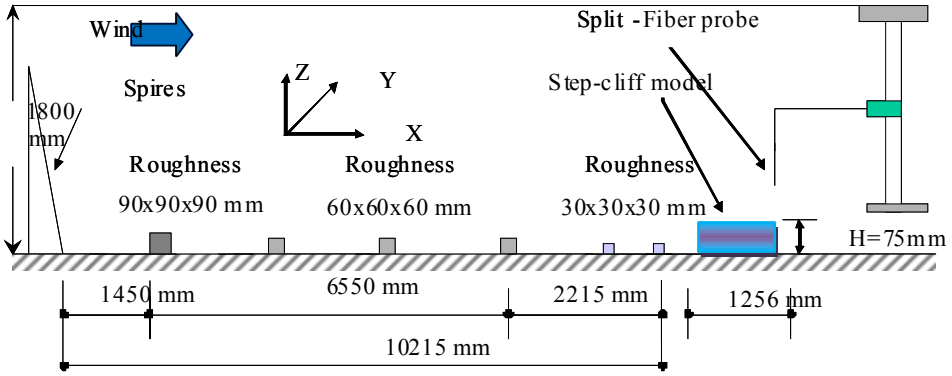

Fig. 3. Schematic diagram of the wind tunnel experimental

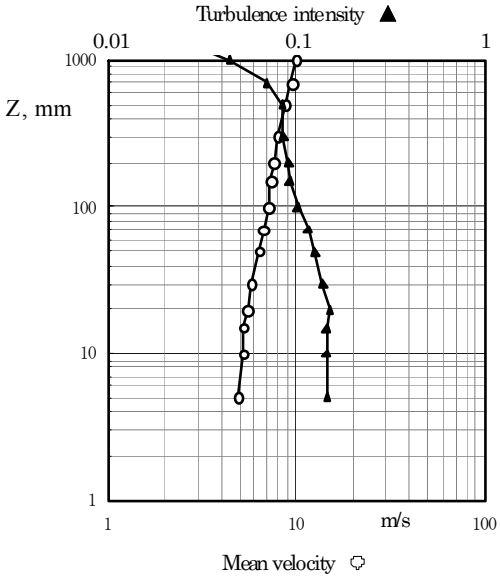

Fig. 4. Vertical distribution of mean velocity and turbulence intensity of incident flow (at X= -800 mm & Y=0)

obstacles fence at X/H=-5, -1, 0.5, 3.8, 7.8 and 11.8. A good agreement between the turbulence models and the wind tunnel experiment was observed for both the surfaces without and with obstacles fence. A slight difference between the turbulence models and the wind tunnel experiments for the surface without obstacles fence was observed at X/H=-5, 7.8 and 11.8 and for the surface with obstacles fence at X/H=-5, and 0.5, which could have been due to the use of three-dimensional isolated step-shaped cliff in the wind tunnel experiment. However, the standard turbulence model was showed to be generally close to the wind tunnel experiments for the surface without obstacles fence.

RESULTS & DISCUSSIONS

The distributions, vectors, and streamlines of the horizontal velocity over the step-shaped cliff model for the rough and smooth surfaces are shown in Figs 9-11. Fig.12 shows the vertical profiles of the mean horizontal velocity over the step-shaped cliff model for the rough and smooth surfaces without at various locations; X/H=-5, -1, 0.5, 3.8, 7.8 and 11.8.

These figures show that the standard and RNG turbulence model predict similar wind velocities over the step-shaped cliff model, except for the smooth surface at 1<Z/H<1.75. The most intensive movement

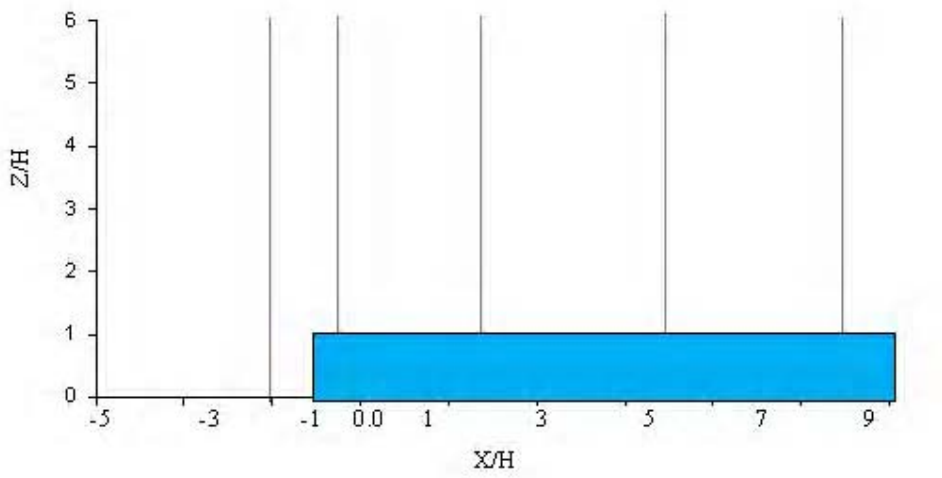

Fig. 5. Sketch of the different locations for the vertical profiles on step-cliff model

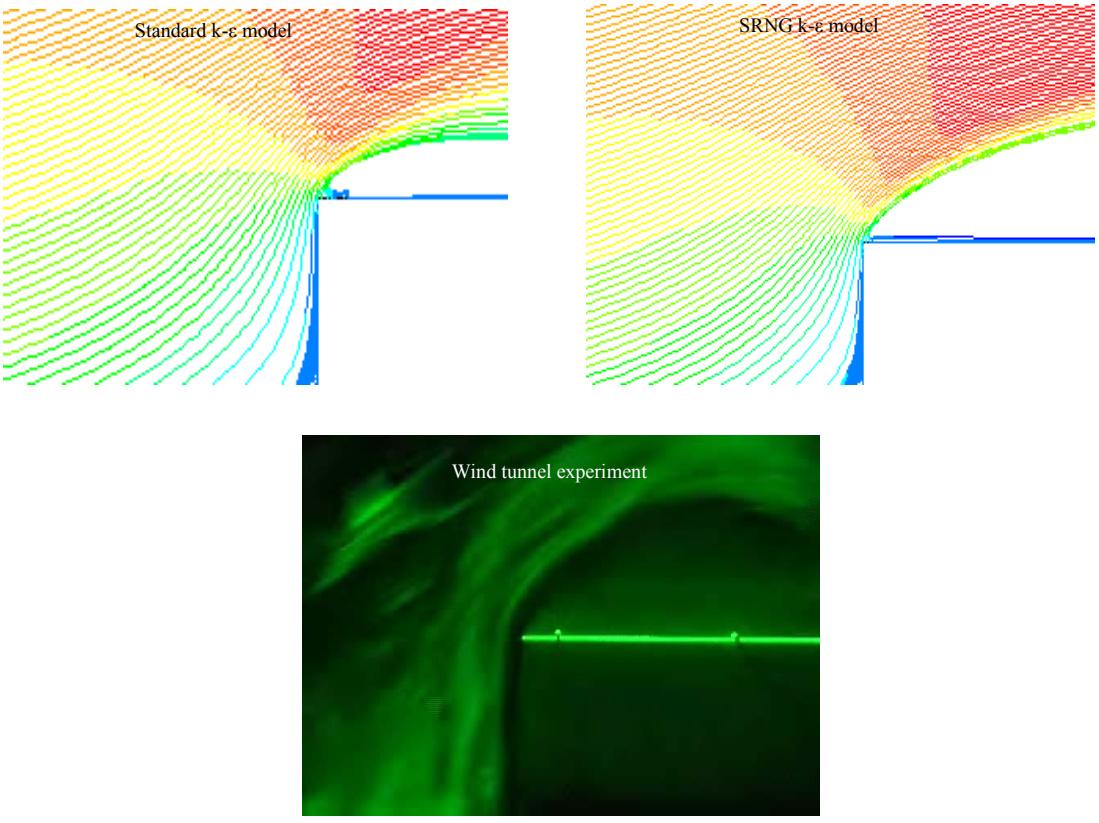

Fig. 6. Flow visualization and streamlines around the frontal corner of the step-cliff model

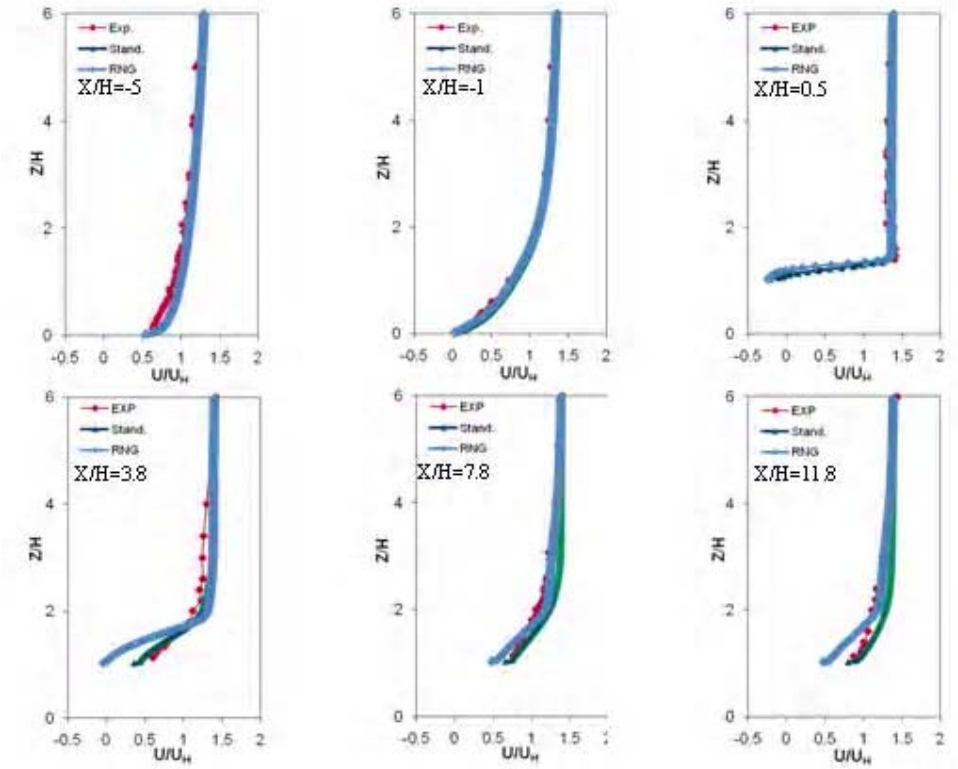

Fig. 7 .Vertical profiles of normalized horizontal velocity over step-cliff model without windbreak fence at

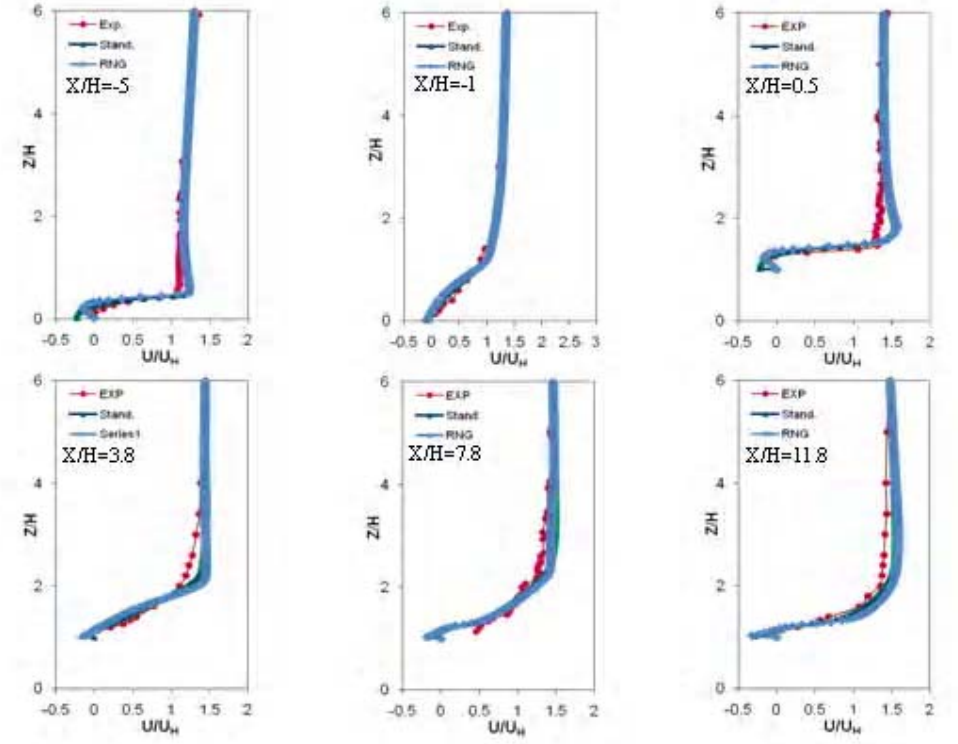

Fig. 8. Vertical profiles of normalized horizontal velocity over step-cliff model with windbreak fence at different locations X/H

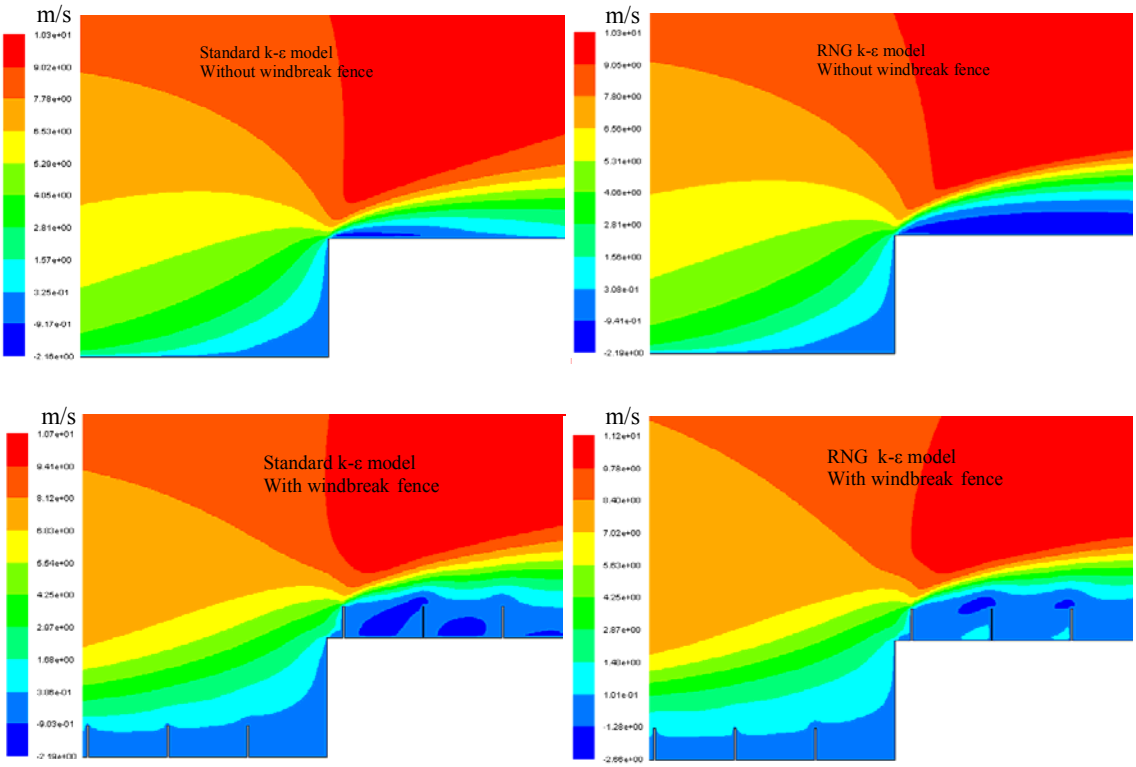

Fig. 9. Mean horizontal velocity distributions over the step-cliff model

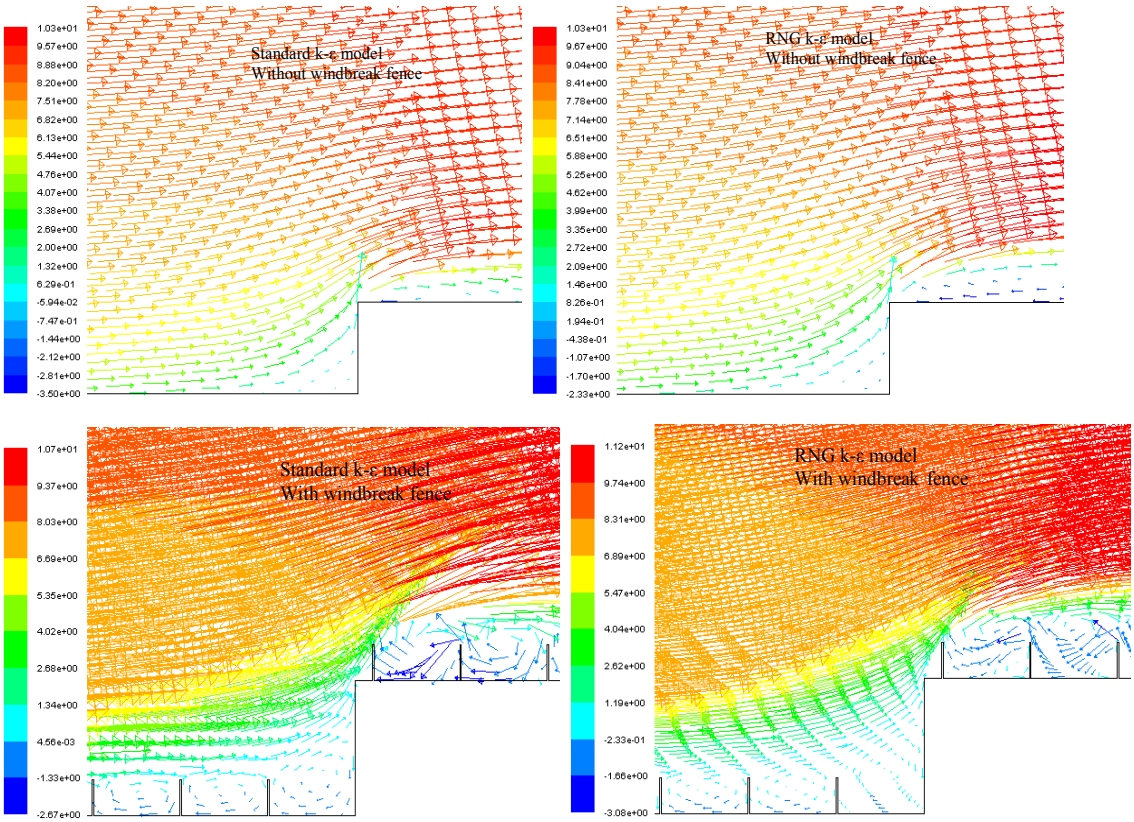

Fig. 10. Mean horizontal velocity vectors over the step-cliff model

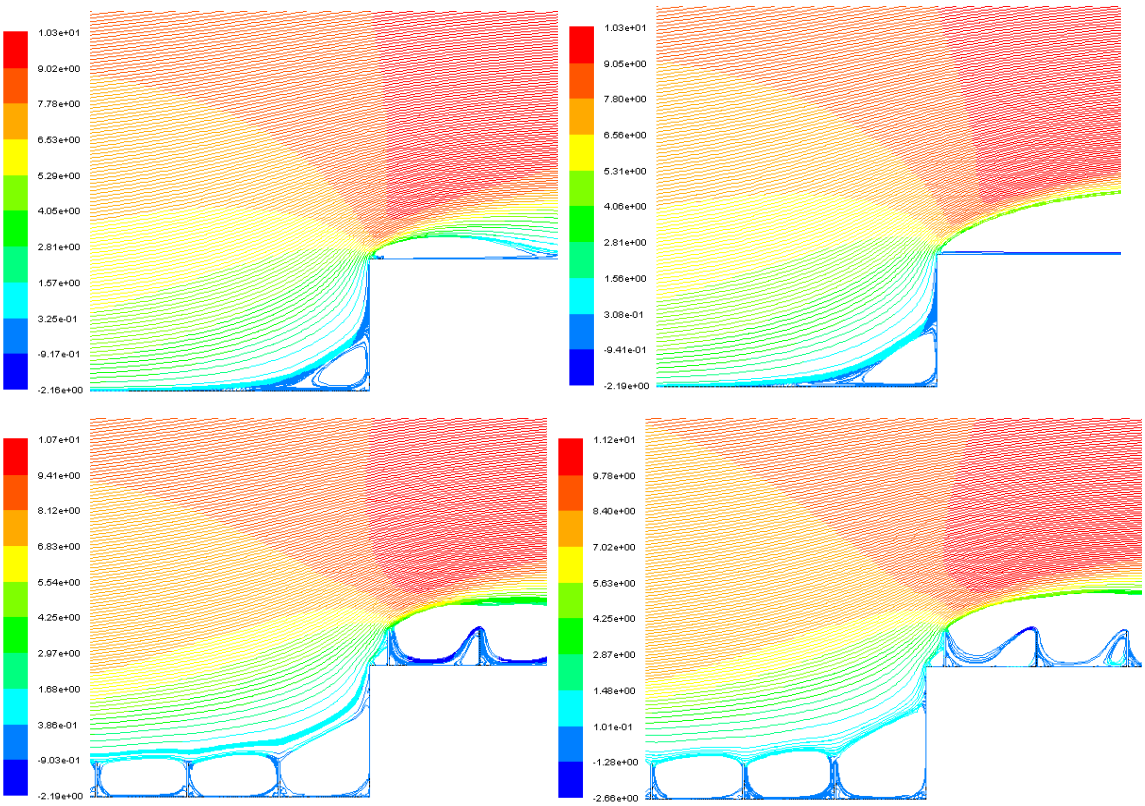

Fig. 11. Streamlines of the mean horizontal velocity over the step-cliff model

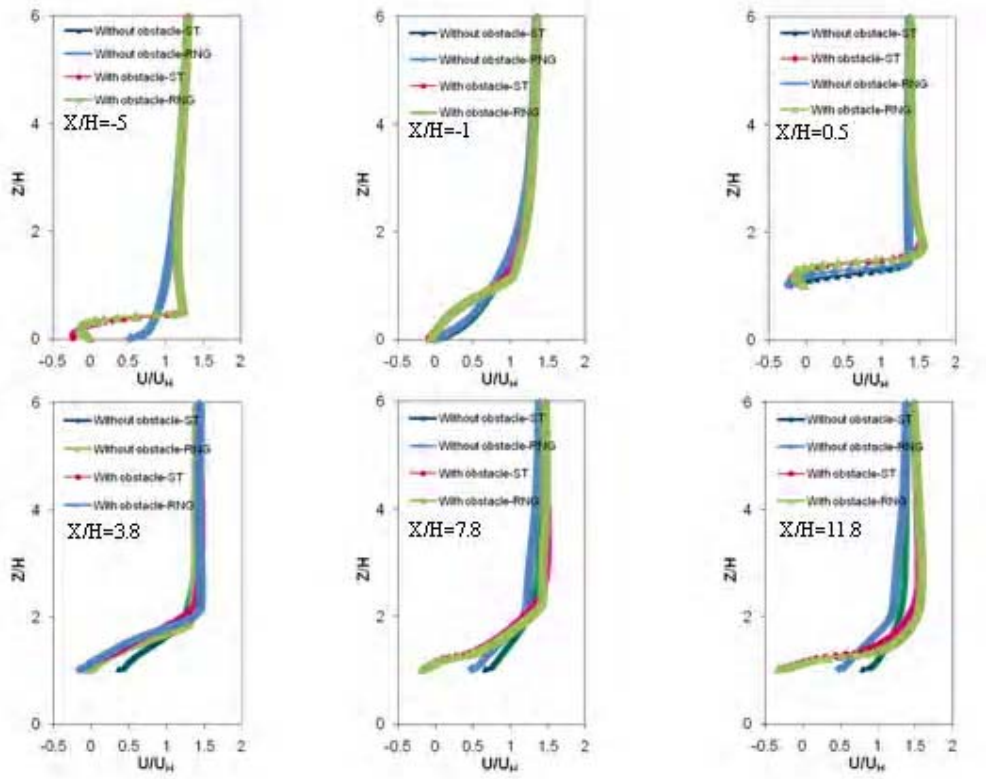

Fig. 12. Vertical profiles of normalized horizontal velocity over step-cliff model at different locations

of the flow appeared near the windward corner of the step-shaped cliff. The mean horizontal velocity appeared to be very small at the windward corner of the step-shaped cliff. The vortex appeared to be rotating clockwise on the step-shaped cliff rough surface between every windbreak fences and for the smooth surface near the ground windward of the step-shaped cliff. The vortex was generated by standard turbulence model was observed smaller than that by RNG turbulence model. A negative velocity was found for the surface with obstacles fence. This meant that the air movement associated with the vortex-like motion effectively towards both the leeward and windward of the windbreak fences in the step-shaped cliff. The wind velocity adjacent for the smooth surface was higher than that for the rough surface of the step-shaped cliff. Flow separation at the windward corner of the step-shaped cliff for the smooth surface was quite small if present at all, and compared to the rough surfaces. Relatively large flow separations were formed by the windbreak fences. The difference between the smooth and rough surfaces was relatively small at Z/H>2. A thick internal boundary layer was generated by the rough surface. Inversely, internal boundary layer for the smooth surface was very thin because there was no windbreak fence. While, at X/H= 0.5, the thick internal boundary layer was generated over the smooth surface compared to the other due to the turbulent mixing, which was formed by the distortion of flow at the windward corner of the step-shaped cliff. The maximum velocity was observed at X/H= 0.5 for the smooth and rough surfaces. This was because the windward corner generated the separation flow. The previous results showed that the rough surface has a great influence on the flow characteristics and vortex rotating.

Besides the mean velocity, it is of interest to know how turbulence might be modified as the flow goes over the step-shaped cliff model. Turbulence structures behind two-dimensional hill are poorly understood.Figs 13-14 show the contours of the turbulence intensity over the step-shaped cliff model for the smooth and rough surfaces. The vertical profiles of the turbulence intensity over the step-shaped cliff model for the smooth and rough surfaces at various locations; X/H=-5, -1, 0.5, 3.8, 7.8 and 11.8 are shown in Fig.14. Vigorous turbulent mixing was observed in the upper part of the frontal corner of the step-shaped cliff model. The turbulence intensity over the rough surface appeared to have similar patterns at Z/H<2. While, the turbulence intensity over the smooth surface appeared to have similar patterns on the step-shaped cliff surface at X/H=3.8, 7.8 and 11.8 for Z/H<2 respectively. The turbulence intensity varied slowly with height. Over the step-shaped cliff, there was significant high intensity near the surface and this led to a large increase in the turbulent stress. There was a strong gradient in the turbulence intensity at X/H=0.5 with the maximum magnitude close to the step-shaped cliff surface. A region of high-turbulence intensity appeared to be along the shear layer downstream of the step-shaped cliff model. Peak values of the turbulence intensity created in the zones were characterized by the highest velocity gradients. The turbulence intensity showed higher value at Z/H<2 over the step-shaped cliff for the smooth surface due to the steep gradient of the velocity than that of the rough surface. The value of the turbulence intensity over the step-shaped cliff at X/H= 3.8, 7.8 and 11.8 for the rough surface was larger than that for the smooth surface.

The turbulent kinetic energy is one of the most important variables in the atmospheric boundary layer. Figs. 15-16 show the contours and vertical profiles of the turbulent kinetic energy over the step-shaped cliff model for the smooth and rough surface surfaces. It is showed that an increase in wind velocity significantly decreases the turbulent kinetic energy over the step-shaped cliff model. The distribution of the turbulent kinetic energy quantifies the turbulent diffusion along the shear layer and is consistent with the direction of the mean flow. The turbulent energy for the rough and smooth surfaces had similar pattern at Z/H>2. The peak value of the turbulent energy appeared to be near the windward corner at X/H=0.5 for the surface without obstacles fence and was considered to be closely related to the small separation as described above. The minimum value of the turbulent energy for the surface without an obstacle fence was displayed at X/H=-5. The values of turbulent energy appeared to be slightly higher at Z/H<2 for the rough surface than that for the smooth surface, except at X/H=0.5 due to the large velocity gradient.

CONCLUSION

A two-dimensional computational fluid dynamics (CFD) model with the standard and RNG k-ε turbulence models were used to investigate the effects of the smooth and rough surfaces on the atmospheric flow over two-dimensional step-shaped cliff model using FLUENT code. The validation of the numerical model was evaluated and agreed with wind tunnel data. The validation of the numerical simulation through the wind tunnel experiment enhances the aspect that numerical simulations, which are a low-cost tool able to provide in reasonable time accurate results regarding fluid dynamics problems. The current study clearly indicates that there is significant influence of the smooth and

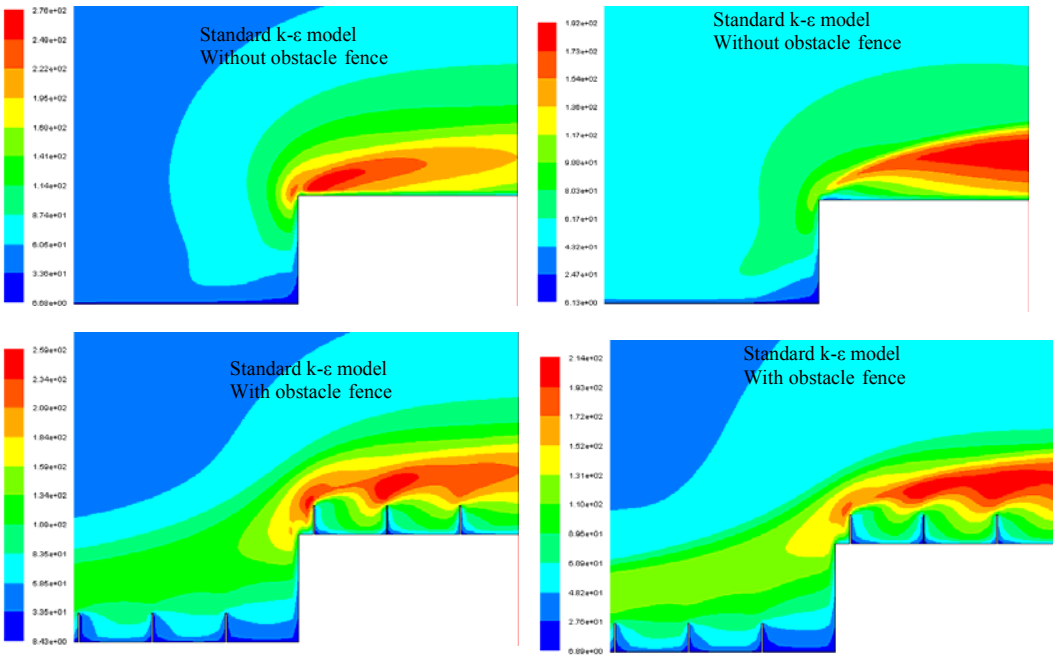

Fig. 13. Turbulence intensity distributions over the step-cliff model

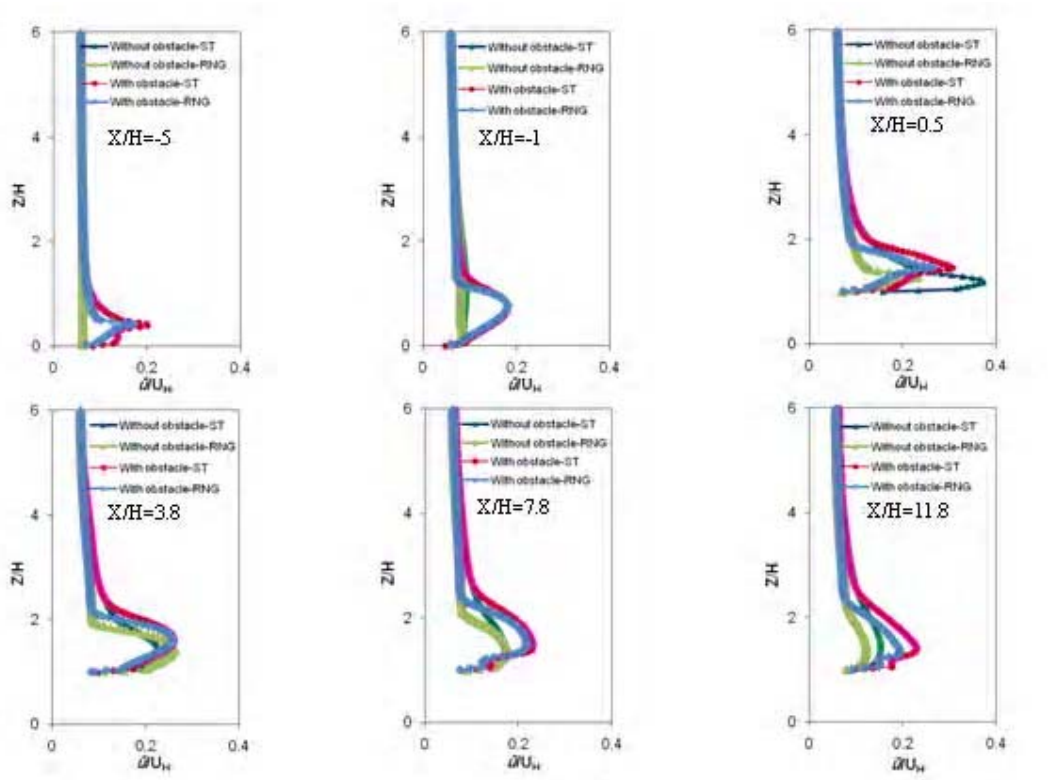

Fig. 14. Vertical profiles of normalized turbulence intensity over step-cliff model at different locations

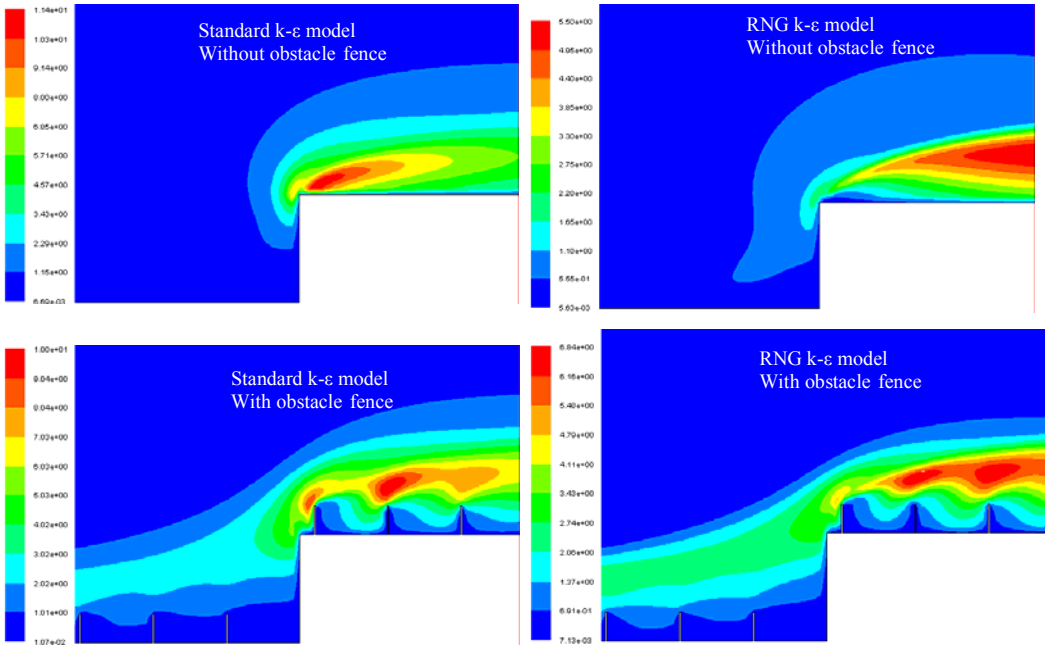

Fig. 15. Turbulent kinetic energy, *K* distributions over the step-cliff model

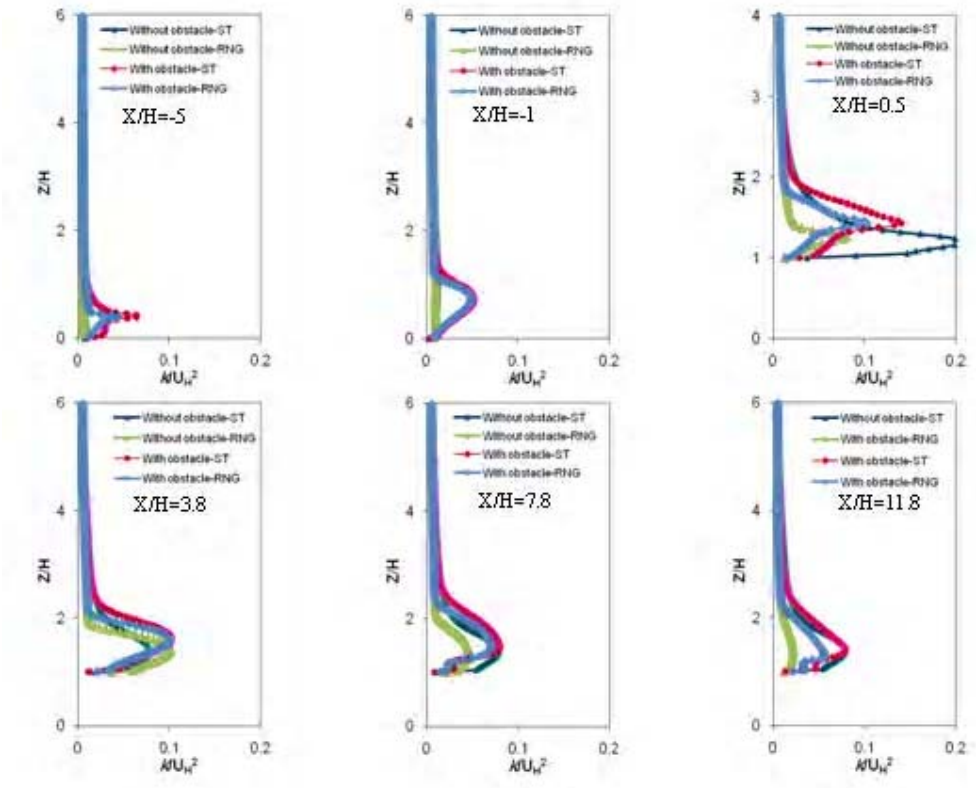

Fig. 16. Vertical profiles of normalized turbulent kinetic energy, *K* over step-cliff model at different locations

rough surfaces on the wind flow over the step-shaped cliff model, the following conclusions can be made:

(a) For mean velocity field, the most intensive movement of the flow appeared near the *windward corner* of the step-shaped cliff. The mean horizontal velocity appeared to be very small *at the windward corner* of the step-shaped cliff. The vortex appeared to be rotating clockwise on the step-shaped cliff surface for the *rough* surface between every windbreak fences and for the *smooth* surface near the ground *windward* of the step-shaped cliff. Inverse flow was found with the *rough* surface. *The wind velocity adjacent to the smooth surface was higher than that of the rough surface* of the step-shaped cliff. *A thick internal boundary layer* was generated by the obstacles fence.

(b) For turbulent field, vigorous turbulent mixing was observed in the upper part of the frontal corner of the step-shaped cliff model. The turbulence intensity varied slowly with height. A region of high-turbulence intensity appeared to be along the shear layer downstream of the step-shaped cliff surface. Peak values of the turbulence intensity created in the zones were characterized by the highest velocity gradients. The turbulence intensity showed higher value at Z/H<2 in the step-shaped cliff for the *smooth* surface. An increase in wind velocity significantly decreases the turbulent kinetic energy over the step-shaped cliff model. The distribution of the turbulent kinetic energy quantifies the turbulent diffusion along the shear layer and is consistent with the direction of the mean flow. The peak value of the turbulent energy appeared to be near the windward corner at X/H=0.5 for the smooth surface. The minimum value of the turbulent energy for the *smooth* surface was displayed at X/H=-5.

REFERENCES

Adams, E. W. and Johnston, J. P. (1988). Effects of the Separating Shear Layer on the Reattachment Flow Structure. Exp. Fluids, **6**, 493-499.

Beljaars, A., Walmsley, J. and Taylor, P. (1987). A mixed spectral finite difference model for neutrally stratified boundary layer flow over roughness changes and topography. Boundary-Layer Meteorol., **38**, 273–303.

Blocken, B., Stathopoulos, T. and Carmeliet, J. (2007). CFD simulation of the atmospheric boundary layer: wall function problems. Atmospheric Environment **41,** 238-252.

Bowen, A. J., and Lindley, D. (1977). A Wind Tunnel Investigation of the Wind Speed and Turbulence Characteristics Close to the Ground over Various Escarpment shapes. Boundary Layer Meteorology, **12**, 259-271.

Djilali, N. and Gartshora, I. S. (1991). Turbulent Flow around a Bluff Rectangular Plate. Part 1: Experimental Investigational. J. of Fluid Engineering, Trans. of ASME, **113 (3)**, 51-59.

Eaton, J. K. and Johnston, J. P. (1981). A Review of Research on Subsonic Turbulent Flow Reattachment. AIAA Journal, **19 (9)**, 1093-1100.

FLUENT Inc. (2010). FLUENT 6.3.16 user Manual.

Friedrich, R. and Arnal, M. (1990). Analyzing turbulent backward-facing steep flow with lowpass-filtered navier-stokes equations. Journal of Wind Engineering and Industrial Aerodynamics, **35**, 101-128.

Ishihara, T., Hibi, K. and Oikawa, S. (1999). A wind tunnel study of turbulent flow over a three-dimensional steep hill. J. of Wind Eng. and Indus. Aerodyn., **83**, 95-107.

Jackson, P, and Hunt, J. (1975). Turbulent wind flow over a low hill. Q J Roy Meteorol Soc., **101,** 929–955.

Kasagi, N. and Matsunaga, A. (1993). Turbulence measurement in a separated and reattaching flow over a backward-facing step with the aid of three-dimensional particle tracking velocimetry. Journal of Wind Engineering and Industrial Aerodynamics, **46**, 821-829.

Krogstad, P. A. and Nickels, T. B. (2006). *Turbulent boundary layer with a step change in surface roughness.* 13th International Conference on Fluid Flow Technologies, 6-9 September 2006, Budapest, Hungary.

Launder, B. E. and Spalding, D. E. (1974). The numerical computation of turbulent flows. Comp. Meth. Appl. Mech. Eng., **3**, 269-289.

Loureiro, J. B. R. and Silva Freire A. P. (2005). Experimental Investigation of Turbulent Boundary Layers over Steep Two-dimensional Elevations. J. of the Braz. Soc. of Mech. Sci. & Eng., **27 (4)**, 329-344.

Mason, P. and Stykes, R. (1979). Flow over an isolated hill of moderate slope. Q J Roy Meteorol Soc., **105**, 383–395.

Olsson, L. (1999). Steps towards an environmentally sustainable transport system. The Science of the Total Environment, **235**, 407-409.

Patankar, S. V. (1980). Numerical heat transfer and fluid flow. McGraw-Hill.

Poggia, D. Katulb, G., Albertsonc, J. D and Ridolfid, L. (2007). An experimental investigation of turbulent flows over a hilly surface. Physics of Fluids, **19 (3)**, 036601-036612.

Ross, A. N., Arnold, S., Vosper, S. B., Mobbs, S. D., Nixon, N. and Robins, A. G. (2004). A comparison of wind-tunnel experiments and numerical simulations of neutral and stratified flow over a hill. Boundary Layer Meteorology, **113**, 427-459.

Taylor, P.A., Walmsley, J. and Salmon, J. (1983). A simple model of neutrally stratiûed boundary-layer ûow over real terrain incorporating wave number-dependent scaling. Boundary-Layer Meteorol., **26**, 169–189.

Walmsley, J. and Taylor, P. (1996). Boundary-layer flow over topography: impacts of the Askervein study. Boundary Layer Meteorol., **78**, 291–320.

Walmsley, J., Taylor, P. and Keith, T. (1986). A simple model of neutrally stratified boundary layer flow over complex terrain with surface roughness modulations . Boundary Layer Meteorol., **36**, 157–186.

William, A. G. and Joseph, B. K. (2000). Behavior of flow over step topography, American Meteorological Society. April, 1153-1164.

Wood, N. (1995). The onset of separation in neutral, turbulent flow over hills. Boundary Layer Meteorol., **76**, 137–164.

Yassin, M. F., Kato, S., Ooka, R., Murakami, S., Takahashi, T. and Ohtsu, T. (2001). Wind tunnel study on prediction of wind characteristic over local topography for suitable site of wind power station (part 3): turbulent characteristics of flow over a two dimensional step model. Summaries of technical papers of annual meeting, AIJ.